USING CONJUNCTION ANALYSIS METHODS FOR MANOEUVRE DETECTION

J. Herzog[(1)]**, H. Fiedler**[(1)]**, and T. Schildknecht**[(2)]

[(1)]*Deutsches Zentrum für Luft- und Raumfahrt, Münchener Str. 20, D-82234 Weßling, Germany,* {*johannes.herzog, hauke.fiedler*}*@dlr.de*

[(2)]*Astronomical Institute, University of Bern, Sidlerstrasse 5, CH-3012 Bern, Switzerland, Email: schildknecht@aiub.unibe.ch*

ABSTRACT

Operational satellites in the geostationary orbit region (GEO) have to perform station keeping manoeuvres to maintain their longitude and inclination. When maintaining an object catalogue, these manoeuvres lead to difficulties within the object identification process. It is possible that the catalogue contains multiple instances of the same object, depending on whether the new observations could be associated to the correct catalogued object. Efficient manoeuvre detection may reduce the number of duplicate objects by connecting orbits after a manoeuvre with those before.

In this work, methods traditionally used for determining collision probabilities were applied to identify manoeuvres. It will be shown that with these methods, manoeuvres may be detected shortly after they were performed. Two orbits and their osculating epochs are taken and the time interval in between the epochs is scanned for a possible close approach. A collision probability is calculated for each epoch and criteria to conclude whether a manoeuvre took place are developed.

In the present study, manoeuvres of the operational satellites Meteosat-8, -9, -10, and -11 are identified and compared to the ones provided by the operating entity, EUMETSAT. This validation of the algorithm is based on the osculating elements before and after the manoeuvre, as well as epoch of the manoeuvres provided by EUMETSAT.

Finally, some time intervals are analysed with orbits based on observations obtained by optical telescopes. These observations were provided by the Astronomical Institute of the University of Bern. It is shown how multiple instances of an object in a catalogue are reduced by using this method.

Key words: Manoeuvre Detection; Conjunction Analysis.

1. INTRODUCTION

When building up a catalogue of objects orbiting around the Earth, observations of active satellites will also be included. Operational satellites will perform station-keeping manoeuvre to ensure proposed operations. As manoeuvres will lead to different orbital elements than calculated with an orbit propagation, new observations of satellites might not be associated to these satellites, and stored into the catalogue as newly detected objects, eventually.

To avoid false storages, a method has to be developed which links observations to satellites despite manoeuvres. An orbit determination will most likely fail, because the orbits before and after a manoeuvre are different. Earlier studies analysed two-line element (TLE) data to identify manoeuvre epochs [e. g. 6]. In those studies, orbital elements are compared to identify most probable manoeuvre epochs. TLE sets are updated regularly and are publicly available [see 8], so the availability of TLE sets of satellites may be considered as an advantage.

In the present study, we took a different approach as we may not have orbital data in the density of TLE sets. In future, the orbits will base on observations acquired by the telescope network SMARTnet^{TM} [see e. g. 5] built up by the German Aerospace Center (DLR). Although a global network is proposed, observations of a specific satellite may not be able to be taken, due to poor weather conditions or technical issues. Orbital elements may not be determined on a regular basis, consequently.

To date, operator data of four geostationary satellites is used to calibrate the method. These orbits are provided by EUMETSAT [see 2] and are related to their meteo satellites Meteosat-8, -9, -10 and -11, respectively. Calibration includes definition of parameters and their intervals for known manoeuvres. The parameters were then tested on epochs without manoeuvres to verify the success of the method.

In the following sections, we will describe the used method as well as results and possible applications to observations.

2. CONJUNCTION ANALYSIS APPROACH

2.1. General Remarks

As a simplification, we assume instantaneous manoeuvres, where the orbit of a satellites is changed immediately. Referring to Soop [7], this assumption is valid when the exact change of orbital elements and applied velocity differences are not analysed. In this case, we might identify one single manoeuvre epoch instead of a time interval.

Assuming an instantaneous manoeuvre, the satellite is on both orbits at the same time. This scenario is similar to an encounter, where two objects are on two diffenrent orbits, but at the same time one the same position. Consequently, a manoeuvre may be analysed with conjunction analysis methods.

A commonly used quantity in conjunction analysis is the encounter probability. In general, it depends on the orbits of the objects involved. But these orbits carry uncertainties of the orbital elements resulting in uncertainties of the calculated positions and velocities.

In the work of Alfano [1], the position uncertainties are connected to the encounter probability. These uncertainties are assumed to be Gaussian distributed around the nominal position, uncorrelated and constant during the close approach or encounter, respectively. The encounter region is an ellipsoid, whose semi-principle axes are equal to n times the position uncertainties (σ), called n-σ covariance ellipsoid. The covariances are assumed to be uncorrelated, so they are summed to form one, large, combined covariance ellipsoid around the primary object, called combined n-σ covariance ellipsoid [for details see again 1]. Values of n are typically chosen to be between three and eight to accommodate conjunction probabilities on confidence levels between $97.071\,\%$ and $99.999\,999\,\%$.

The satellites are assumed to be spherical, and the secondary object describes a tube-shaped path. If this path touches or crosses the combined n-σ covariance ellipsoid, a close approach takes place. As an additional condition, when the smallest distance between both satellites is smaller than the sum of their radii, they collide.

2.2. Encounter Probability

For the calculation of the maximum probability for an encounter, amongst those mentioned above the following quantities are needed: The size of the combined object, r_{OBJ}, is set to the sum of the radii of both satellites. The relative distance of the closest approach is set to $d_{\min}$.

The combined n-σ covariance ellipsoid is projected onto a plane, whose normal vector points into the direction of the relative velocity vector between both satellites. It can be shown, that the projection of an ellipsoid onto a plane is always an ellipse [see e. g. 4]. The sizes of its semi-major and the semi-minor axes depend on the semi-principle axes of the combined n-σ covariance ellipsoid and of the orientation of the relative velocity vector, respectively. Let a be the semi-major and b the semi-minor axis of the projected ellipse, the aspect ratio then becomes:

$$q_{\text{AR}} = \frac{a}{b}.$$

In Alfano [1], there are given several approximate solutions for the maximum probability, $P_{\max}$, and its associated minor-axis standard deviation, σ_x, respectively. The focus in the present study lies on the first-order approximation in both cases, see Eqns. (1) and (2).

In case of manoeuvres, some of the assumptions above simplify. The same satellite is considered before and after the manoeuvre, so the size of the combined object is twice as large as the satellite. Consequently, the combined n-σ covariance ellipsoid is twice as large as the n-σ covariance ellipsoid.

Referring to Flohrer et al. [3], the position uncertainties for objects in the geostationary ring are $359\,\mathrm{m}$ in radial direction, $432\,\mathrm{m}$ in the direction of motion and $86\,\mathrm{m}$ out-of-plane. A factor of $n = 5$ is chosen to be above a $99.99\,\%$ confidence level. The individual 5-σ covariance ellipsoids are summed and result in a combined 10-σ covariance ellipsoid.

2.3. Scanning Method

When two orbits are given, the time interval between the reference epochs will be investigated. Both element sets are propagated to an epoch t between both reference epochs. The relative distance between both calculated positions and the corresponding probability are calculated. The Eqns. (1) and (2) are modified and the minimum distance, $d_{\min}$, is replaced by the relative distance at epoch, $d(t)$. Consequently, the probability $P^{(1)}$ is not the maximum encounter probability anymore, but the probability at the epoch t, with the associated minor-axis standard deviation at that epoch, displayed in Eqns. (4) and (3).

This way, one gets a development of the probability with time, $P^{(1)}(t)$. The maximum probability gives the most likely epoch of the manoeuvre. Besides the maximum of the probability, its distinction is important. Another maximum close by can make the decision harder or even impossible whether a manoeuvre took place.

To identify the suspected manoeuvre epoch and the corresponding encounter probability as exact as possible, the time steps of the scan interval are not constant, but get smaller with higher encounter probability. It follows the

$$\sigma_x^{(1)} = \sqrt{\frac{\left(q_{\mathrm{AR}}^2+1\right)\cdot r_{\mathrm{OBJ}}^2 + 2d_{\mathrm{min}}^2 + \sqrt{\left(q_{\mathrm{AR}}^2+1\right)^2\cdot r_{\mathrm{OBJ}}^4 + 4d_{\mathrm{min}}^4}}{8q_{\mathrm{AR}}^8}} \tag{1}$$

$$P_{\mathrm{max}}^{(1)} = \frac{r_{\mathrm{OBJ}}^2}{16q_{\mathrm{AR}}^3\left(\sigma_x^{(1)}\right)^4}\cdot\exp\left(-\frac{1}{2}\left(\frac{d_{\mathrm{min}}}{q_{\mathrm{AR}}\cdot\sigma_x^{(1)}}\right)^2\right)\cdot\left(8q_{\mathrm{AR}}^2\left(\sigma_x^{(1)}\right)^2 - \left(q_{\mathrm{AR}}^2+1\right)\cdot r_{\mathrm{OBJ}}^2\right) \tag{2}$$

$$\sigma_x^{(1)}(t) = \sqrt{\frac{\left(q_{\mathrm{AR}}^2+1\right)\cdot r_{\mathrm{OBJ}}^2 + 2d(t)^2 + \sqrt{\left(q_{\mathrm{AR}}^2+1\right)^2\cdot r_{\mathrm{OBJ}}^4 + 4d(t)^4}}{8q_{\mathrm{AR}}^8}} \tag{3}$$

$$P^{(1)}(t) = \frac{r_{\mathrm{OBJ}}^2}{16q_{\mathrm{AR}}^3\left(\sigma_x^{(1)}(t)\right)^4}\cdot\exp\left(-\frac{1}{2}\left(\frac{d(t)}{q_{\mathrm{AR}}\cdot\sigma_x^{(1)}(t)}\right)^2\right)\cdot\left(8q_{\mathrm{AR}}^2\left(\sigma_x^{(1)}(t)\right)^2 - \left(q_{\mathrm{AR}}^2+1\right)\cdot r_{\mathrm{OBJ}}^2\right) \tag{4}$$

equation:

$$\Delta t = \frac{\left|\log_{10}\left(P^{(1)}(t)\right)\right|}{500}\cdot 1\,\mathrm{d}$$

2.4. Peak Contrast of the maximum Encounter Probability

If the encounter probability reaches a maximum, one wants to know if this peak is distinct. A decision whether a manoeuvre took place might be made by the maximum encounter probability itself, but the distinction of a peak is a more reliable criterion. Furthermore, the estimation of the manoeuvre epoch will only be possible, when the peak is distinct and no other maximum reaches the same order of magnitude. Here, the measure of distinction is the peak contrast, and is defined as the logarithmic ratio of the highest encounter probability, $p_{1^{\mathrm{st}}}$, to that of the second highest peak, $p_{2^{\mathrm{nd}}}$, respectively:

$$\mathcal{P} = \log_{10}\left(\frac{p_{1^{\mathrm{st}}}}{p_{2^{\mathrm{nd}}}}\right) \tag{5}$$

With this definition, $\mathcal{P}$ is always non-negative. A value of $\mathcal{P}$ equal to zero leads to two peaks of the same height. A value $\mathcal{P} = 1$ represents an encounter probability which is ten times higher than the second highest peak.

3. ANALYSIS

Before analysing manoeuvres, a distinction in parameter space between manoeuvres and non-manoeuvres has to be made. In the present study, the parameter space consists of the encounter probability p and the peak contrast, $\mathcal{P}$.

Three kinds of analyses have to be performed in order to achieve decisive criteria:

1. intervals with orbital elements of two different objects,
2. intervals where no reported manoeuvre took place,
3. finally, intervals with reported manoeuvres.

The first analysis will prove that the results of scans with orbital elements of two different objects will not be confused with manoeuvres.

The second analysis will prove that the results of scans without a manoeuvre differ significantly from those with manoeuvres, considering the same object.

The company EUMETSAT operates several meteo satellites, and provides manoeuvre announcements and orbital elements on a regular basis [cf. 2]. These sets of orbital elements and manoeuvre epochs build the data set of the analysis.

The element sets were propagated and the encounter probabilities were determined for each epoch. Afterwards, the probabilities of the two highest peaks were used to determine the peak contrast of the maximum encounter probability.

3.1. Different Objects

In case of two perfect geostationary objects (circular orbit with vanishing inclination), the distance between both stay constant over time. In the same manner, the encounter probability remains constant and on low level. Consequently, there is no distinct peak expected ($\mathcal{P} \approx 0$).

In reality with orbital evolution, uncertainites in position and velocity and analemma-shaped subsatellite trajectories, orbits will deviate from perfect circularity and will show inclination. Therefore, there will be maxima of the encounter probability, although still on low level. The

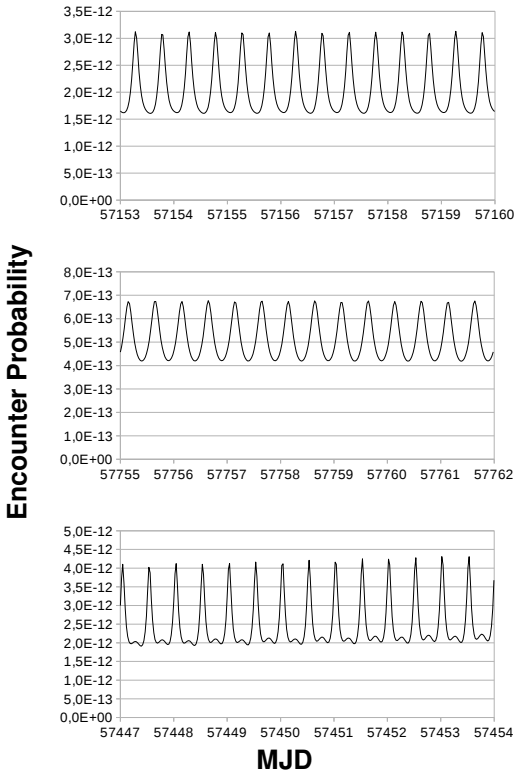

Figure 1. Examples of results from scans of two different orbits; note the linear y-axis in contrast to the graphs in Fig. 3

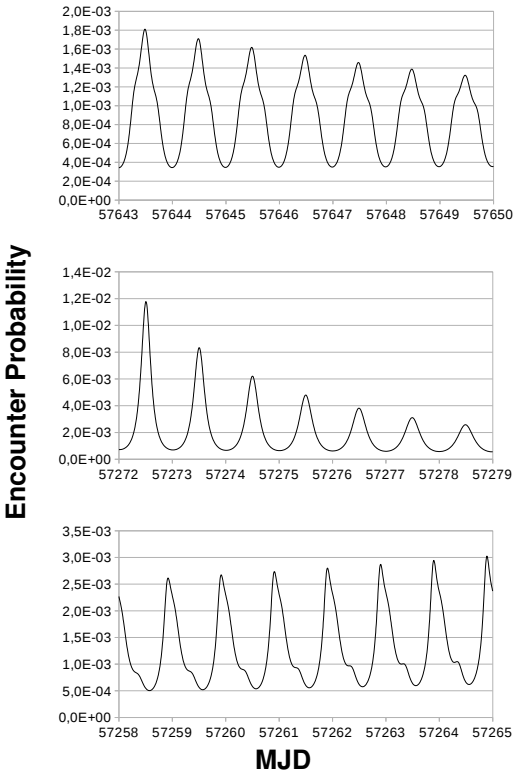

Figure 2. Examples of results from scans of intervals without reported manoeuvres; note the linear y-axis in contrast to the graphs in Fig. 3

value of $\mathcal{P}$ stays around zero, because each maximum will be in the same order of magnitude.

Based on these considerations, it is expected that the results of those scans will be located in an area in the $p - \mathcal{P}-$parameter space with low encounter probability and low $\mathcal{P}$ value.

In practise, two different objects with an orbital element set each is used. As the osculating epochs are one week apart in most cases, the orbital element sets were also taken with one week between them. In general, the difference may also be set to a larger margin to increase the data set.

Figure 1 shows three examples of those scans. The encounter probability values stay in the same order of magnitude during the entire analysis interval.

In Fig. 4, the results are displayed as black crosses. The peak probability is smaller than 10^{-8} and the variation of the encounter probability is small, all values are in the same order of magnitude during the analysis interval. Maximums of the encouter probability are also in the same order of magnitude, displayed by peak contrast values lower than 1.

3.2. Intervals without Manoeuvres

Taking two orbital element sets from one object but focussing solely on intervals without reported manoeuvres, the encounter probability of a single orbit is analysed. In case of a perfect geostationary object, the positions are equal over time, and the encounter probability is expected to be one. Again, there is no distinct peak expected $(\mathcal{P} \approx 0)$.

In reality, mostly due to uncertainties from the orbit determination process, the encounter probability will deviate from one with a non-vanishing $\mathcal{P}$ value.

Based on these considerations, it is expected that the results of those scans will be located in an area in the $p - \mathcal{P}-$parameter space with high encounter probability but low $\mathcal{P}$ value.

Figure 2 shows three examples of those scans. The encounter probability values stay in the same order of magnitude during the entire analysis interval, but it is significantly higher than those from different orbits.

In Fig. 4, the results are displayed as red circles. The peak probability is larger than 10^{-6} but the variation of the encounter probability is small, all values are in the same order of magnitude during the analysis interval. Max-

imums of the encouter probability are also in the same order of magnitude, displayed by peak contrast values lower than 1.

3.3. Analysis of given Manoeuvres

Finally, two orbital element sets are taken, for which in between a manoeuvre took place. A manoeuvre epoch was given by the operator for these manoeuvres.

Of the aforementioned satellites Meteosat-8, -9, -10 and -11, a total of 46 East-West station-keeping (EWSK) and 3 North-South station-keeping (NSSK) manoeuvres were analysed. They are scattered within a time interval between May 2014 and December 2016.

Figure 3 shows two examples of scans. The osculating epochs are the beginning and the end of the scan interval, respectively. Figure 3(a) shows an East-West station-keeping manoeuvre of Meteosat-8, while Fig. 3(b) shows a North-South station keeping manoeuvre of Meteosat-10. The maximum encounter probability of Meteosat-8 is about 6.8×10^{-4}, but more important the peak contrast of the peak is about 5.3. The manoeuvre of Meteosat-11 has a maximum encounter probability of about 1.9×10^{-6} with a peak contrast of about 2. The developed method is applicable to both kinds of manoeuvre, although the maximum encounter probability is orders of magnitudes smaller and the peak contrast is also smaller.

Figure 4 shows the distribution of the peak contrast values over maximum encounter probabilities. The blue squares represent scans of EWSK manoeuvres and the light blue diamonds represent NSSK manoeuvres. The red circles are the results of scans without manoeuvres. There is a clear distinction between manoeuvres and no manoeuvres. The red solid line represent the maximum limit to exclude the possibility of a manoeuvre while the thick blue solid line represent the minimum limit to claim a manoeuvre being detected, respectively. Based on the current data set, the peak contrast $\mathcal{P}$ must fulfil the condition

$$\mathcal{P} \leq \frac{2}{7} \cdot \log_{10}(p) + 2,$$

where p is the maximum encounter probability, to exclude the possibility of a manoeuvre. This equation was not derived through a fit but as such that all current results are below the line.

The results of EWSK manoeuvre scans alone form a line in $p - \mathcal{P}-$space. It might be again described as $\mathcal{P} = a \cdot \log_{10}(p) + b$, with the following fit parameters:

$$a = 1.01 \pm 0.07$$
$$b = 7.37 \pm 0.17$$

To claim a manoeuvre being detected the peak contrast $\mathcal{P}$ has to fulfil the following condition:

$$\mathcal{P} \geq 1.01 \cdot \log_{10}(p) + 7.37 - 5 \cdot \sqrt{(0.07 \cdot \log_{10}(p))^2 + 0.17^2}, \quad (6)$$

when $p \geq 10^{-8}$. This means the lower level to claim a manoeuvre to be detected is the -5σ-level of the fitted line. There is no upper limit for claiming, because very distinct maximums may occur at lower peak probabilities in future analyses and must not eliminated at this early stage.

Although there are no measurements in the area between both limits lines, this may happen when investigating future manoeuvres. The parameters themselves may be adjusted as well.

Results of scans of two different orbits are located in an intervall $p \leq 10^{-8}$ and $\mathcal{P} \leq 1$. They fill a different area in $p - \mathcal{P}-$space and may be distinguished very well from the other events.

4. CONCLUSION

In this paper, we presented a study concerning manoeuvre detection of geostationary satellites. Two sets of orbital elements of a parent object were used, and the time interval between the osculating epochs was scanned. Each orbit was represented by one pseudo-object, the manoeuvre of the parent object was then interpreted as a close encounter between both pseudo-objects. Main criteria were the highest encounter probability and the distinction of the highest peak of the temporal distribution of the probabilities.

The method was developed and tested with operator data. These data constisted of a state vector at an osculating epoch together with satellite's mass and reflectivity coefficient. Manoeuvres and intervals without manoeuvres were analysed to achieve parameters with make a distinction possible.

5. OUTLOOK

Next step is to use the developed method and analyse orbits based on observations. This way it is possible to include this method into a filtering process to associate new observations with catalogued objects. After a manoeuvre, those associations might not be possible without further information about the manoeuvre. Apart from few companies this information is not publicly available.

An open topic is the used arc lengths for the orbit determination. On one hand, small uncertainties are required and therefore a large observation arc; on the other hand a manoeuvre should quickly be detected after it happened and therefore the arc has to be short. One will have to

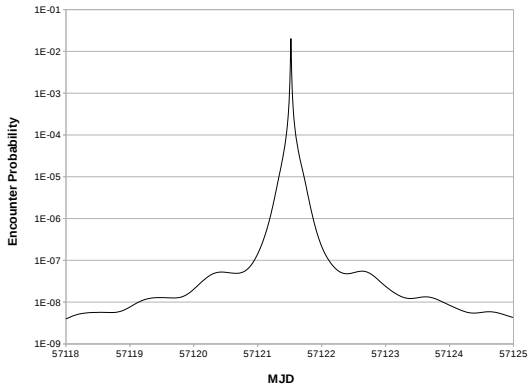

(a) Meteosat−8, EWSK

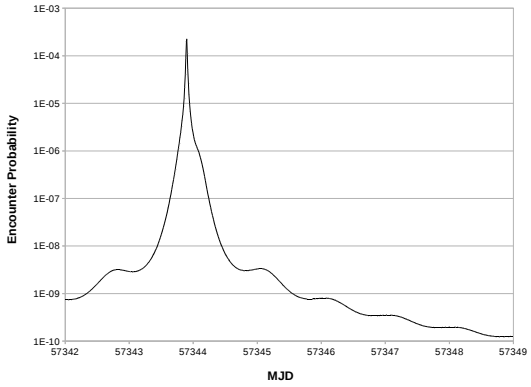

(b) Meteosat−9, EWSK

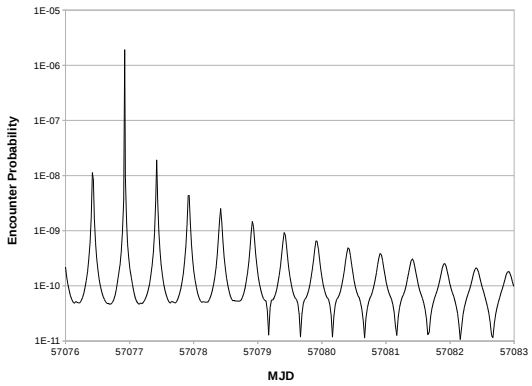

(c) Meteosat−10, NSSK

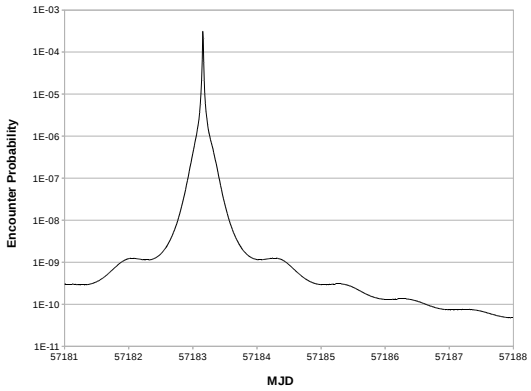

(d) Meteosat−10, EWSK

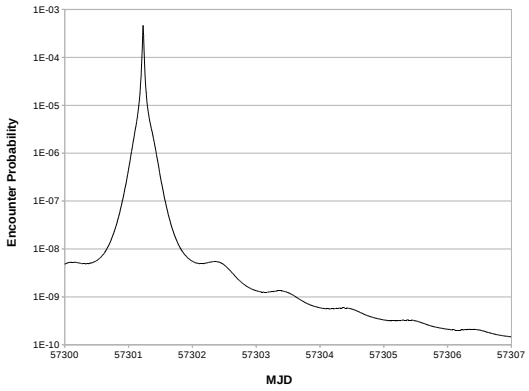

(e) Meteosat−11, EWSK

Figure 3. Examples of scans for manoeuvre

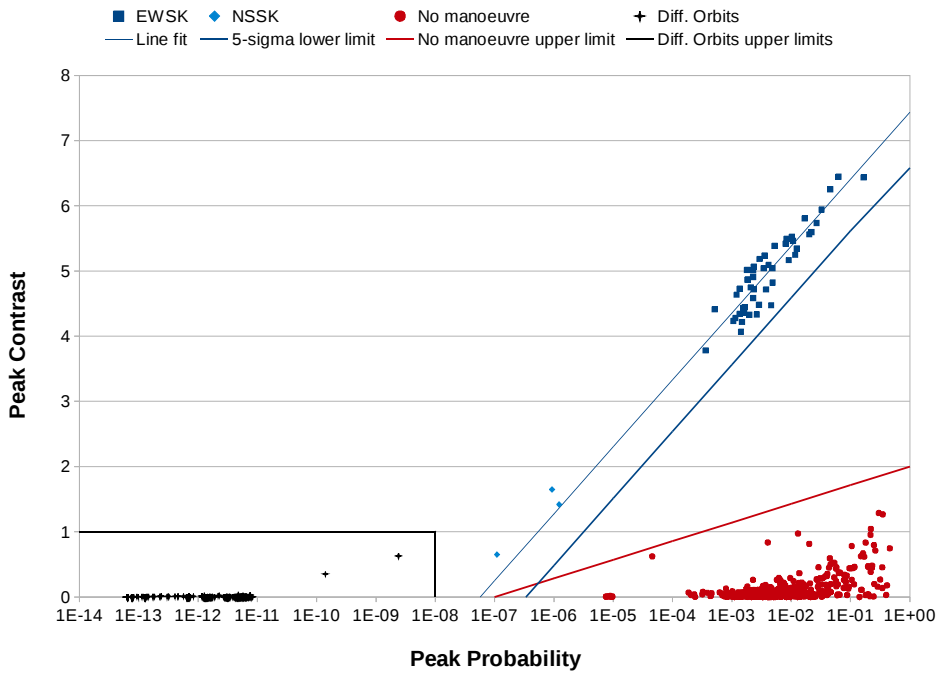

Figure 4. Distribution of calculated peak contrasts with respect to their maximum encounter probability; blue squares: East-West station-keeping (EWSK) manoeuvres, blue diamonds: North-South station-keeping (NSSK) manoeuvres, red circles: intervals without manoeuvres, black crosses: two different orbits

find a compromise, especially after the manoeuvre. Furthermore, the assumed position uncertainties for the covariance ellipsoids might not represent each and every geostationary object. They will be exchanged by results based on our orbit determination.

The osculating epochs of the orbital elements sets were mostly seven days apart. When using optical observations this might most likely not be the case. It has to be further analysed how the parameters will be affected.

REFERENCES

1. Alfano, S.: Relating Position Uncertainty to Maximum Conjunction Probability. The Journal of the Astronautical Sciences, No. 2, Vol. 53, 193-205, 2005
2. EUMETSAT: Orbital data. retrieved 20/2/2017
3. Flohrer, T., Krag, H., Klinkrad, H.: Assessment and Categorization of TLE Orbit Errors for the US SSN Catalogue. Proceedings of the Advanced Maui Optical and Space Surveillance Technologies Conference, 2008
4. Gendzwill, D.J. and Stauffer, M.R.: Analysis of Triaxial Ellipsoids: Their Shapes, Plane Sections, and Plane Projections. Mathematical Geology, No. 2, Vol. 13, 135-152, 1981
5. Herzog, J., Fiedler, H., Weigel, M., Montenbruck, O., Schildknecht, T.: SMARTnet: A Sensor for Monitoring the Geostationary Ring. Proceedings of the 24$^{\text{th}}$ International Symposium on Space Flight Dynamics, 2014
6. Kelcey, T., Hall, D., Hamada, K., Stocker, D.: Satellite Maneuver Detection Using Two-line Element (TLE) Data. Proceedings of the Advanced Maui Optical and Space Surveillance Technologies Conference, 2007
7. Soop, E.M.: Handbook of Geostationary Orbits. Microcosm, Inc. Torrance (USA); Kluwer Academic Publishers Dordrecht Boston London, 1994
8. SPACE-TRACK.ORG: TLE data sets of unclassified objects. retrieved 20/2/2017